Effect of water mist on temperature and burning velocity of stretched propane-air premixed flames

A. Yoshida[1], Y. Momomoto[1], H. Naito[2] & Y. Saso[3]
[1]*Department of Mechanical Engineering, Tokyo Denki University, Japan*
[2]*Fire and Disaster Management Agency, Tokyo, Japan*
[3]*National Research Institute of Fire and Disaster, Tokyo, Japan*

Abstract

Effects of fine water mist on the flame temperature and laminar burning velocity of propane/air premixed flame were investigated by using a single jet-plate configuration. For the case without water mist, the measured laminar burning velocities are in reasonably good agreement with previously reported data and numerical simulation. The dependence of the burning velocity on the stretch rate for the case without water mist is positive for all mixtures tested, resulting in the negative Markstein length, which coincides with previous experimental and theoretical studies. With water mist addition, the laminar burning velocity is lowered significantly and its dependence on the stretch rate is changed to negative. This leads to apparently positive Markstein lengths. Concurrently, the flame temperature decreases linearly with the water mist mass loading. Also, it decreases with the stretch rate, even if the water mist mass loading is kept constant. The positive Markstein length was discussed on the basis of the mist droplets behavior in the stagnation flow field. Even if the mist mass loading is kept constant, the mist droplets do not follow the diverting flow field when the stretch rate is high and the droplets accumulation occurs in the stagnation region where the burning velocities were measured. This fact results in the lower burning velocity and lower flame temperature as compared to those measured for uniformly dispersed water mist.
Keywords: water mist, fire extinguishment, stagnation flow, burning velocity, Markstein number, stretch rate.


WIT Transactions on Engineering Sciences, Vol 79,
www.witpress.com, ISSN 1743-3533 (on-line)
doi:10.2495/MPF130191

1 Introduction

Halon 1301 (trifluoroboromomethane, CF_3Br), a most popular halogenated hydrocarbon, was known to be effective in fire suppression and was widely used [1]. However, since the ban on the production of fire suppression agents containing bromine in 1987, the search for alternative fire suppressants has been motivated to establish their effectiveness and to understand the fire suppression mechanism of the new agents both for premixed flame [2, 3] and diffusion flame [4, 5]. Among newly suggested fire suppression agents, water mist has many advantages as it is inexpensive, ubiquitous, non-electrically conductive and nontoxic [6, 7]. Additionally, water mist imposes no environmental problems. Furthermore, it can be used to suppress various kinds of fires with water quantities much less than sprinklers and hence can reduce collateral damage.

Water has favourable physical properties for fire suppression. Its high heat capacity and high latent heat of evaporation can absorb a significant quantity of heat from flames. Water also expands 1400 times when it evaporates to vapor, which results in the dilution of the surrounding oxygen concentration. With the formation of fine water mist, its effectiveness in fire suppression is increased due to the significant increase in the surface area of water that is available for heat absorption and evaporation. Therefore, the primary mechanisms of extinguishment should be due to heat extraction and oxygen displacement. Additionally, the extinguishment can be achieved by removing a certain amount of chain carrying or branching radicals and water mist was found to have such a chemical effect on the laminar burning velocity [8].

Laminar burning velocity is a fundamental property of a flammable gas mixture describing the overall reaction rate, heat release, and heat and mass transport in the flame, and as such the reduction in laminar burning velocity is frequently used as an indicator of the effectiveness of an inhibiting agent [2, 3, 8]. In addition, diffusion flames often have a stabilization region at their bases that is premixed, and good correlation has been found between the reduction in burning velocity and the concentration of inhibitors to extinguish a diffusion flame [9].

So far, several techniques for measuring the one-dimensional laminar burning velocity have been used for wide range of temperature, pressure and fuel, and rather accurate measurements have been obtained by employing flat or curved flames in stagnation flow [10], propagating spherical flames in combustion vessel [11, 12], flat flames stabilized on burner [13] or conical flames stabilized on a Bunsen burner [14]. With all those measurement techniques proper care could be taken to remove the effect of flame stretch either during experimentation or through further data processing. The counterflow, opposed-jet technique is well documented [15, 16], and it has been traditionally implemented with the use of two opposed, aerodynamically contoured nozzles. However, this technique includes jet and flame stability, significant fuel consumption, and complex upper burner design in order to avoid overheating. Although these problems might be resolved, the use of the lower burner and a plate could be a simpler method since a very stable flame is obtained, less fuel is

used, and the upper burner can be eliminated. In a twin-flame or single-flame configuration, the minimum is identified in the velocity profile as a reference upstream burning velocity S_L and the velocity gradient a ahead of the minimum point is used to obtain the stretch rate K experienced by the flame, K being -(1/2)a for a cylindrical stagnation flow. Using this technique, the unstretched laminar burning velocity S_L^0 is obtained by systematically determining the dependence of the upstream reference burning velocity S_L on the stretch rate K and extrapolating the data to zero K [17]. A linear or non-linear extrapolation to zero stretch yields the unstretched laminar burning velocity S_L^0 [18]. The recent investigation [10] has shown that the single jet-plate configuration results in laminar burning velocities that are identical to the ones obtained by the twin-jet configuration at low stretch rates; at these low stretch rates, the flame is located away from the plate and downstream heat losses minimally affect flame propagation. Therefore, it is clear that at low stretch rates, the presence of the plate does not affect the S_L values, although the limit at extinguishment K_{ext} is reduced significantly by the heat loss to the stagnation plate [19].

There is a fairly good agreement between values obtained by different measurement techniques. This clearly demonstrates an improvement in consistency, and this is due to the recognition of the influence of stretch and the resulting corrections for it.

In this study, the stagnation flow field was established by using a jet emerging from a nozzle and impinging on a water-cooled stainless steel plate to investigate the effect of the water mist on the flame temperature and laminar burning velocity of propane/air mixture at low and intermediate stretch rate. The unstretched laminar burning velocity S_L^0 was obtained by a linear extrapolation to zero stretch. The stagnation plate temperature was not precisely controlled in the present study, because it has been found that as long as finite heat loss is present, the critical stretch rate at extinguishment is not sensitive to the heat loss and the effect of plate temperature is not as important [19].

2 Experimental apparatus

2.1 Burner with single jet-plate configuration

The implementation of the counterflow, opposed-jet techniques for the determination of laminar burning velocities and stretch rates at extinguishment has been reported in detail [10, 15–19]. The single jet-plate configuration included the replacement of the upper burner with a stainless steel plate. The experimental apparatus, shown in Fig. 1, consisted basically of an axisymmetric burner and an axisymmetric plate. The axis of the burner was vertical and the upward jet impinged on the horizontal plate. The design of the plate allowed the constant plate temperature with cooling water. To ensure that the experimental results were not affected by the specific nature of the stagnation plate, the cooled plate was replaced by an uncooled ceramic plate. However, the minimum velocity at the flame and the burned gas temperature immediately after the flame were not changed. Boundary layer effects were also found to be negligible as

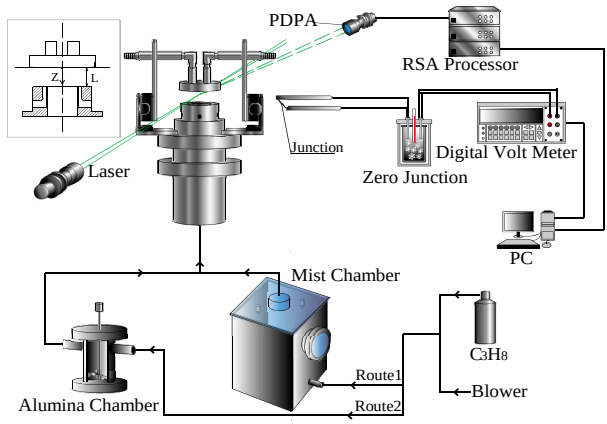

Figure 1: Experimental apparatus.

long as the flame is not too close to the stagnation plate. Since velocity measurements were conducted by using phase Doppler particle analyser (PDPA), the plate was chamfered with a slant of 3 degrees to enable the laser beams to make the closest approach on the flame near the plate. The plate was mounted on a traverse system to allow easy and accurate movement relative to the burner. The burner and plate assembly was mounted on another traverse system, whereas the PDPA system was stationary.

A laminar flat flame was required. Therefore, the flow at the exit of the burner needed to be uniform and free of turbulence. Special care was taken in the design of the burner in order to achieve these objectives. The burner had a settling chamber to reduce the flow disturbance. The settling chamber contained three damping screens of fine mesh. The nozzle had a smooth reduction of area to enable a uniform velocity profile at the exit. The inside diameter of the nozzle exit was 45 mm. The combustible mixture stream was surrounded by a shroud flow of air and was protected from the disturbances caused by the surrounding air entrained by the outcoming jet. This air flow also blew off the secondary diffusion flame which was caused on the periphery of the primary premixed flame especially when the mixture composition was rich.

Propane was used as a fuel throughout. The flow rates of the air and the fuel were measured by respective rotameters calibrated before experiments. The flow rate of the shroud air was measured by another rotameter and was controlled to ensure the stable laminar flat flame at the central portion of the stagnation flow.

The PDPA requires the presence of light scattering particles in the flow. For the case without water mist, the mixture flow was seeded with aluminum oxide, Al_2O_3, by a particle generator through route 2 in Fig. 1. These particles, of mean diameter around 1.0 μm, are suitable for using in PDPA in reactive flow because of their stable physical and chemical properties. The entire mixture flow went through the particle generator. When the water mist was added to the mixture flow through route 1 in Fig. 1, the mist droplets themselves played a role of light scattering particles and aluminum oxide particles were not seeded.

The temperature was measured by an R-type thermocouple of 50 μm in diameter. Catalytic effect was eliminated by silica-coating of the junction and wire elements. The thermocouple was mounted on a transverse mechanism.

2.2 Water mist generator

In the present study, pure water was used for producing water mist. To generate a fine water mist, 6 piezoelectric atomizers were installed in the water mist generator. These atomizers could be operated separately. The water mist flow rate was controlled by the number of units activated. The mixture gas flow was separated into 6 paths in the water mist generator. Each path was bent so that the mixture gas flow swept through the hovering water mist produced on each piezoelectric unit and entrained mist that was then carried up to the exit of the water mist generator. A nominal mist supply rate for one piezoelectric unit was 575 ml/h at 1.6 MHz. For the piezoelectric atomizers, the mist size distribution and the supply rate depend in general on the water level above the unit and the water temperature. Care was taken to maintain the water level, 40 mm above the piezoelectric plate. The mechanical vibration of the piezoelectric plate generates heat that is transferred into the surrounding water, resulting in a slow rise in water temperature. To avoid this effect, water was heated by an electric heater and its temperature was kept constant at 310 K. We confirmed that, for our experiments, temperature changes in water were statistically insignificant. Water mist diameters and their distributions were measured by a PDPA, and the number mean diameter D_{10} was 11.5 μm and the Sauter mean diameter D_{32} was 18.4 μm with a wide range of the size distribution ranging from 1 μm to 50 μm.

3 Experimental results and discussion

3.1 Appearance of flame

The presence of the stagnation plate modifies the pressure field and the velocity profile, producing a slightly dish-shaped flame when it is not close to the stagnation plate. The central portion of the flame, however, can be assumed to be planar and perpendicular to the central stream tube. When the equivalence ratio, $\phi > 1.4$, the cellular instability appeared at small velocity gradient a, for large separation distance L and small uniform ejection velocity u_0 at the nozzle exit. Additionally, when $\phi < 0.7$, the flame was deformed significantly and not stationary at small a. The experimental conditions, therefore, were limited within the range of equivalence ratio, $0.8 < \phi < 1.3$.

3.2 Velocity profile along the stagnation stream line and the burning velocity

The velocity profile along the stagnation stream line can be considered to be the superposition of the effects of the flame and the stagnation flow field. The actual velocity and temperature profiles measured in a propane/air flame are shown in Fig. 2. When approaching the flame zone, the velocity decreases almost linearly

with decrease of the distance from the stagnation plate *z*. The velocity gradient *a* was determined by the slope of the linear part of the velocity profile. The velocity abruptly increases concurrently with temperature in the flame zone, and then decreases again towards the stagnation plate. The velocity at the point of initial temperature rise is the point where the curve starts to depart from the descending line of unburned gas velocity due to thermal expansion. It was determined that this velocity is very close to the minimum velocity in the entire traverse, especially when the velocity gradient *a* is low. It is noted that in the stagnation flow field, the velocity gradient *a* ahead of the flame zone coincides with a half of the lateral stretch rate *K* of the flame zone. The aerodynamic (hydrodynamic) stretch rate *K* was determined from the velocity gradient as $K = -(1/2)(du/dz)$ at the quasilinear part of the profile ahead of the flame, and the minimum point at the location at which the heating starts was determined as a reference upstream burning velocity S_L, similarly to previous investigations by Law and co-workers [10, 16–19]; *u* stands for the axial flow velocity and *z* for the spatial coordinate in the axial direction. The unstretched laminar burning velocity S_L^0 can be subsequently determined by systematically extrapolating the S_L data to zero *K*. Internal stretch due to thermal expansion across the flame zone was neglected as previous studies [16]. By increasing u_0, the uniform ejection velocity from the nozzle, *K* increases, the flames are pushed toward the stagnation plate, and extinguishment is eventually occurred when a critical value K_{ext}, which is defined as the stretch rate at extinguishment, is reached.

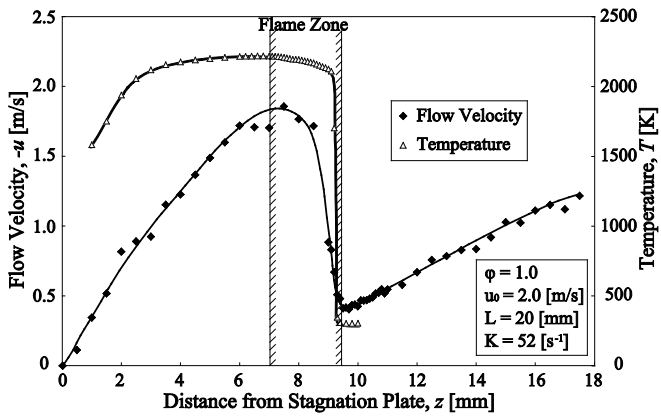

Figure 2: Velocity and temperature distributions without water mist.

3.3 Determination of laminar burning velocity S_L^0

By identifying the minimum point of the velocity profile as a reference upstream burning velocity S_L corresponding to the imposed stretch rate *K* and by plotting S_L versus *K*, the laminar burning velocity without stretch S_L^0, can be determined through linear extrapolation to $K = 0$ in accordance with Ref. 16. Figure 3 shows the values of burning velocity S_L as a function of the stretch rate *K* for

propane/air mixtures. The lines are based on least squares fits of the measured data. The burning velocity S_L increases with the stretch rate K for all mixtures tested. The results of Ref. 20 also exhibit such an increasing tread. For sufficiently weak, off-stoichiometric mixtures, these linear increases terminate abruptly with the occurrence of extinguishment. It is clear that the gradient of each plot increases with the equivalence ratio.

Laminar burning velocity without stretch, S_L^0, is shown in Fig. 4. The numerical simulation of one-dimensional, premixed, unstretched flame was conducted by using the well-established PREMIX code in the CHEMKIN

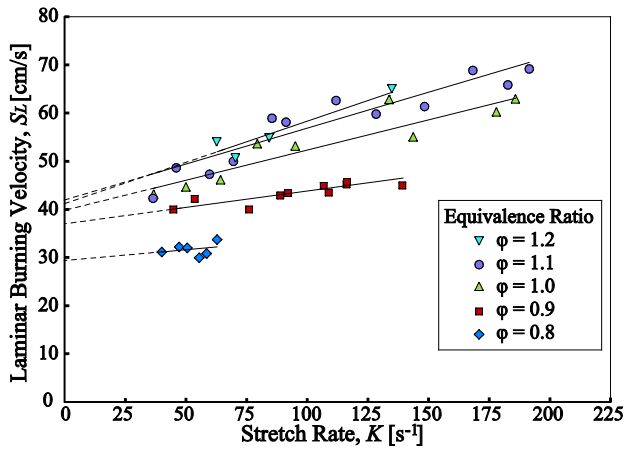

Figure 3: Dependence of the burning velocity S_L on the stretch rate K for propane/air mixtures without water mist.

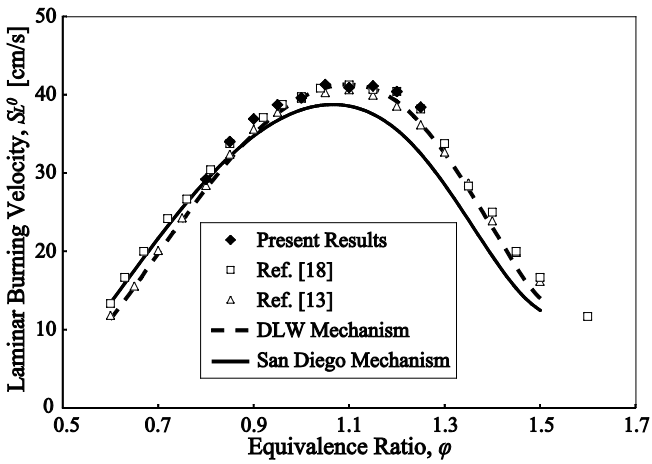

Figure 4: Experimentally and numerically determined unstretched laminar burning velocities, S_L^0, as a function of equivalence ratio, ϕ.

package. The chemical kinetic models for propane oxidization are based on the San Diego mechanism [21] and that proposed by Davis *et al*. [22]. In the San Diego mechanism, 46 chemical species and 235 elementary reactions are considered, whereas 71 species and 469 reactions are included in the DLW mechanism. Figure 4 compares the present experimental data with previous data obtained by using the counterflow configuration [18] and the flat-flame burner [13]. The comparison of experimental data of Refs. [13] and [18] shows good agreement except for the lean side where the data obtained by using the counterflow configuration are slightly higher than those obtained by using the flat-flame burner. However, the difference is considered within the experimental error. Although the present experiment is limited within the range of equivalence of 0.8 and 1.3, the data are generally in reasonably good agreement with those of Refs. [13] and [18], in spite of the fact that the laminar burning velocities were determined by using independent methodologies. The calculated data obtained by adopting the San Diego mechanism are close to the experimental data only on the lean side, whereas on the rich side the calculation predicts lower burning velocities. The DLW mechanism yields a better agreement with the experimental data, although the prediction slightly underestimates the burning velocity on the lean side.

3.4 Characteristics of water mist

The mist size distribution was monitored during experiments to ensure that the mist was uniformly dispersed in the air stream. The mist volume flux measured by the PDPA was primary determination of the amount of liquid water delivered to the flame. Comparison runs between the PDPA determination of the water flow rate and the nominal value reported by the manufacturer revealed that about 10 % of the generated water mist reached the flame zone. The size distribution can be assumed to be log-normal and have a wide size distribution from 1 μm to 50 μm with the number mean diameter of 11.5 μm and the Sauter mean diameter of 18.4 μm.

Since the total amount of water which is atomized in the mist generator depends mainly on the number of piezoelectric units activated, the number density of mist droplets changes with the mixture flow velocity. Therefore, the distance between the burner exit and the stagnation plate L was varied to change the velocity gradient a, keeping the mixture flow velocity u_0 constant to maintain the number density of mist droplets at a desired value.

3.5 Effect of water mist on the laminar burning velocity

When the water mist was added to the air stream, the velocity profile along the stagnation stream line changed as shown in Fig. 5, where the water mist flow rate Q_w is 24.0 ml/min. The local velocity u was measured by PDPA with the water mist as the seeding particles. Similar velocity profiles were obtained for methane/air premixed flames with and without water mist [23]. The flame zone moves closer towards the stagnation plate than the case without water mist as shown in Fig. 2. The constant velocity gradient in the upstream unburned

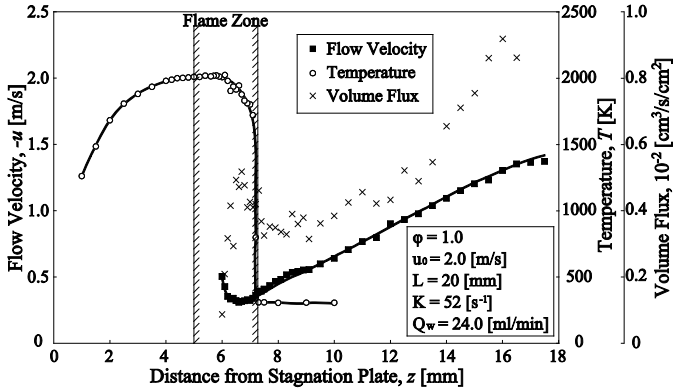

Figure 5: Velocity and temperature distributions and volume flux of water mist.

mixture region was unaffected even if the water mist was added. It is clear that the minimum velocity ahead of the flame zone is lower than that without water mist, suggesting that the laminar burning velocity S_L decreases when the water mist is added in the unburned mixture. It is noted that the point of initial temperature rise does not coincide with the point of the velocity minimum and the velocity increase is delayed somewhat after the temperature rise. The mist size is relatively large as seeding particles for PDPA measurements. The large mist causes large inertial force and cannot follow precisely the abrupt velocity change as in the flame zone. In the flame stabilized in the stagnation flow field, the deceleration in the approach flow changes to acceleration due to thermal expansion, and the inertial force retards the mist acceleration.

Laminar burning velocities S_L for the case with water mist are shown in Fig. 6. We can observe definite deference of the dependence of the burning

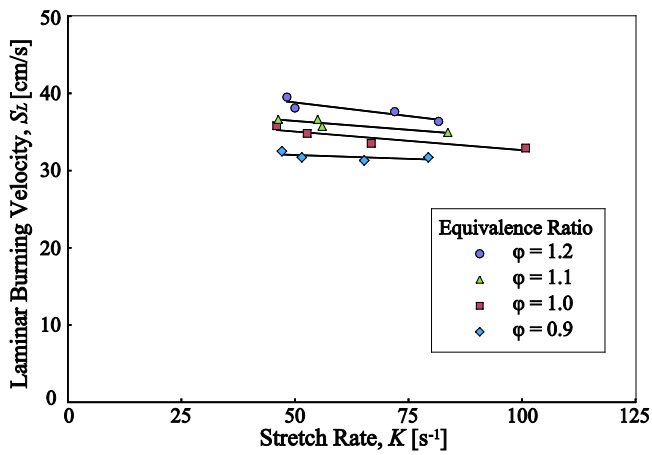

Figure 6: Dependence of the burning velocity S_L on the stretch rate K for propane/air mixtures with water mist.

velocity on the stretch rate. The burning velocity decreases with the stretch rate. The laminar burning velocity S_L^0 without stretch obtained by extrapolating to K = 0 is higher than that without water mist. This fact is in conflict with the thermal consideration; the water mist extracts heat from the flame zone, which should results in a lower burning velocity as compared to that without water mist. Therefore, the apparent high burning velocity at K = 0 is an artifact occurring from the flow field inherent in the stagnation flow. However, it should be noted that if the stretch rate is the same, the burning velocities with water mist are significantly lower than those without water mist.

3.6 Markstein length

Effect of flame stretch on the laminar burning velocity was correlated phenomenologically by Markstein [24] using the Markstein length, as follows, and later it was analysed theoretically by Clavin [25].

$$S_L = S_L^0 - L_m K \tag{1}$$

where L_m is the Markstein length. The plots of S_L as a function of K yield the Markstein length, L_m, which is a function of only equivalence ratio ϕ for the present conditions. Figure 7 shows the Markstein length for the cases with and without water mist. These lines are based on least squares fits of measurements. When the water mist is not added, the Markstein length is always negative, suggesting positive dependence of the burning velocity on the stretch rate. The absolute value of the Markstein length increases with the equivalence ratio. Therefore, the dependence of the burning velocity on the stretch rate increases. The same increasing tread was reported in [20], where the Markstein length was expressed by $-\alpha(\phi)/S_L^0$, and α was plotted against the equivalence ratio ϕ. The

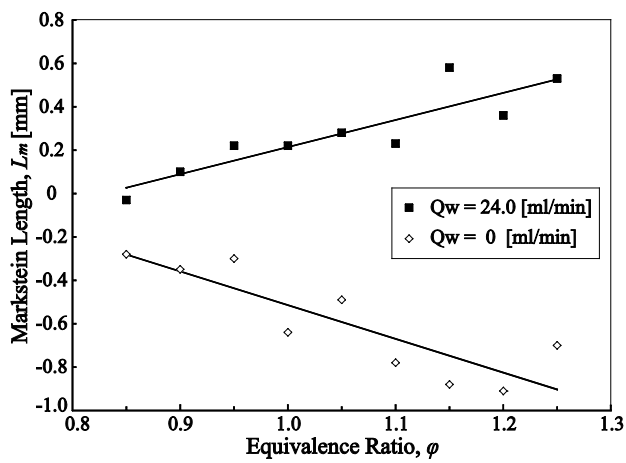

Figure 7: Markstein length with and without water mist.

coefficient α, a function of ϕ, involves the diffusion and Lewis number effects through equivalence ratio. On the other hand, when the water mist is added, the Markstein length changes its sign and has positive values. For this case, the Markstein length increases with the equivalence ratio. In principle, the Markstein length should be a function of diffusivity and Lewis number for gaseous mixtures, which was shown in the theoretical analysis [25]. However, the evaporation process and water vapor should affect the Markstein length in the mist-laden gaseous mixtures.

3.7 Water mist behavior in the stagnation flow field

Water mist contains a number of fine water droplets. Figure 8 shows the velocity of each droplet of respective diameter, u_d. Far from the flame zone, the droplets should have roughly the same velocity as the gas stream. As the gas velocity decreases with approaching the stagnation plate, i.e. z = 15 mm, the equilibrium in velocities between liquid and gas phase is lost. The inertial force is larger for large droplets and the large droplets move faster than the smaller ones in the decelerating flow field. Therefore, the mean velocity of droplets averaged over all sizes is slightly higher than the actual gas phase velocity in the decelerating flow field. With approaching the flame zone, strong acceleration occurs due to thermal expansion and the decelerating flow field changes to the accelerating one through a neutral point. As approaching this point, inertial force decreases and the drag forces act to re-establish the equilibrium in velocities at z = 10 mm. All the droplets become to follow the gas stream with approaching the flame zone where the velocity minimum appears, i.e. z = 6 mm. The point of the velocity minimum of droplets is, however, closer to the stagnation point than that of actual gas phase velocity minimum due to the inertial delay as shown in Fig. 5.

In regimes close to the flame zone where the deceleration changes to acceleration, faster droplets catch up to slower ones, and the volume flux will

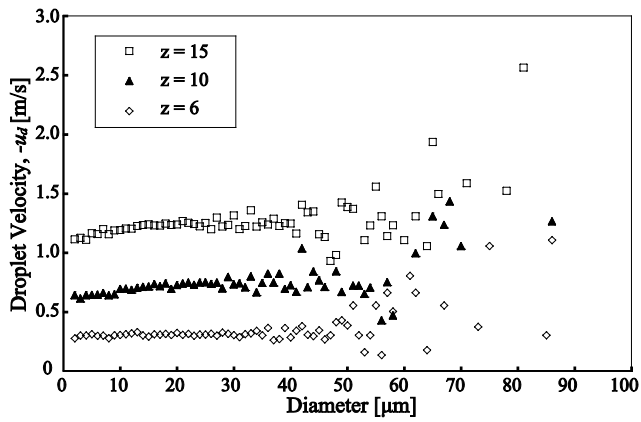

Figure 8: Velocity of each droplet of respective diameter along the stagnation stream line.

tend to rise. In addition, when the velocity gradient a is large, the droplets do not follow the lateral acceleration due to flow divergence. These result in an accumulation of droplets occurring just ahead of the flame zone. This effect contributes to increase the volume flux of mist in the central portion of the flame zone, and as such decreases the laminar burning velocity S_L as compared to that for low velocity gradient case, even though the volume flux of water droplets in the far upstream region is same.

As shown in Fig. 6, when the water mist is added, the laminar burning velocity decreases with increase of the stretch rate. This trend is opposite to that for the case without water mist, resulting in the positive Markstein length. This trend should be apparent, because the volume flux of water mist entering the flame zone increases with increase of the stretch rate.

3.1 Effect of water mist on flame temperature

Figure 9 shows the temperature profiles along the stagnation stream line for cases with and without water mist. There exists a temperature plateau in and beyond the flame zone for all profiles. Therefore, the flame and burned gas are unaffected by the heat loss due to the water cooled stagnation plate. Thus, the plateau temperature is regarded as the flame temperature T_f which should be slightly lower than the adiabatic flame temperature because the conduction loss through thermocouple elements was not corrected. The flame temperature T_f decreases with water mist mass loading. At the flame front, the burning velocity is balanced by the unburned mixture velocity. The laminar burning velocity decreases with the flame temperature. Therefore, the flame moves closer to the stagnation point with the water mist flow rate. The flame thickness is inversely proportional to the laminar burning velocity and as such increases with the water mist mass loading. This fact suggests that the thermal effect of water mist is significant in reducing the laminar burning velocity.

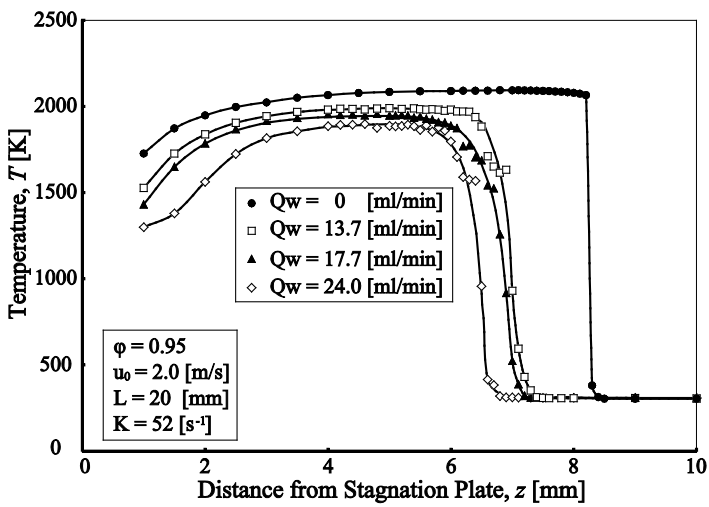

Figure 9: Variations of temperature with water mist flow rate.

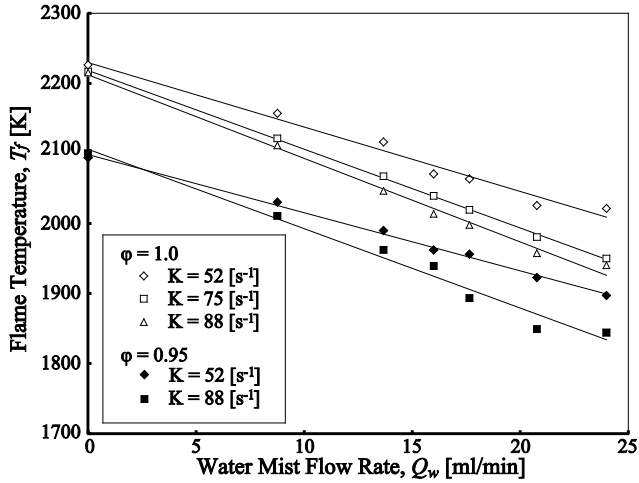

Figure 10: Flame temperature variations with water mist flow rate and stretch rate.

The effect of the water mist flow rate on the flame temperature is shown in Fig. 10 for ϕ = 0.95 and 1.0. For both cases, the flame temperatures for the case without water mist are close to the respective adiabatic flame temperatures. The flame temperature decreases linearly with the water mist mass loading. It is noted that the reduction of the flame temperature depends on the stretch rate. The flame temperature is lower when the stretch rate is large, even if the water mist mass loading is kept constant. As mentioned before, the mist accumulation occurs when the stretch rate is large. These accumulated water mist absorbs more heat from the flame than the low stretch case. Therefore, the effect of water mist in suppressing the flame is affected by the flowfield configuration.

4 Conclusions

In the present study, the effect of fine water mist on the laminar burning velocity of propane/air premixed flame was investigated by using a single jet-plate configuration. Water mist was generated by 6 piezoelectric atomizers and their characteristics were measured by the phase Doppler particle analyzer. Diameter of water mist thus generated was widely distributed, ranging from 1 μm to 50 μm, with the number mean diameter of 11.5 μm and the Sauter mean diameter of 18.4 μm. For the case without water mist, the measured laminar burning velocities were in reasonably favorable agreement with previously reported data obtained by disparate methodologies and also with the results of numerical simulation using the PREMIX code in the CHEMKIN package. When no mist was added, the dependence of the burning velocity on the stretch rate was positive for all mixtures tested, resulting in the negative Markstein lengths. Absolute value of the Markstein length increased linearly with the mixture

equivalence ratio. The laminar burning velocity was lowered significantly by adding the water mist. The large mist has large inertial force compared to drag force and does not follow the stagnation flow field. Such mist is accumulated in front of the flame zone. Accumulation of the water mist is in proportion to the stretch rate, which causes the apparent negative dependence of the laminar burning velocity on the stretch rate, resulting in the positive Markstein number. The flame temperature decreases linearly with water mist mass loading. At the same time, the flame zone moves towards the stagnation plane to accommodate the laminar burning velocity to the mixture flow velocity. The decrease of the burning velocity thickens the flame zone. Additionally, the flame temperature is reduced with the increase of stretch rate. This can be also explained by the water mist accumulation around the stagnation stream line. Therefore, great care must be taken when the stagnation flow field is used to investigate the effect of solid and liquid phase particles on e.g. extinguishment of diffusion flames or burning velocities of premixed flames.

References

[1] Hirst, R. and Booth, K, Measurement of flame-extinguishing concentrations. *Fire Technology*, **13**, pp. 296-315, 1977.
[2] Noto, T., Babushok, V., Hamins, A. and Tsang, W., Inhibition effectiveness of halogenated compounds. *Combust. Flame*, **112**, pp. 147-160, 1998.
[3] Korobeinichev, O.P., Shvartsberg, V.M., Shmakov, A.G., Knyazkov, D.A. and Rybitskaya, I.V., Inhibition of atmospheric lean and rich $CH_4/O_2/Ar$ flames by phosphorus-containing compound. *Proc. Combust. Inst.*, **31**, pp. 2741-2748, 2007.
[4] Papas, P., Fleming, J.W. and Sheinson, R.S., Extinction of non-premixed methane- and propane-air counterflow flames inhibited with CF_4, CF_3H and CF_3Br. *Proc. Combust. Inst.*, **26**, pp. 1405-1411, 1996.
[5] Liu, S., Soteriou, M.C., Colket, M.B. and Senecal, J.A., Determination of cup-burner extinguishing concentration using the perfectly stirred reactor model. *Fire Safety J.*, **43**, pp. 589-597, 2008.
[6] Grant, G., Brenton, J. and Drysdale, D., Fire suppression by water sprays. *Prog. Energy Combust. Sci.*, **26**, pp. 79-130, 2000.
[7] Liu, Z. and Kim, A.K., A review of water mist fire suppression technology: part II-application studies. *J. Fire Protec. Eng.*, **11**, pp. 16-42, 2001.
[8] Yoshida, A. and Yukawa, A., Numerical simulation of the effects of water mist on flame structure and flame speed of propane-air premixed flame, *Proc. 9th ASPACC*, submitted, 2013.
[9] Hastie, J.W., *High Temperature Vapors: Science and Technology*, Academic Press: New York, p. 332, 1975.
[10] Vagelopoulos, C.M. and Egolfopoulos, F.N., Direct experimental determination of laminar flame speeds. *Proc. Combust. Inst.*, **27**, pp. 513-519, 1998.
[11] Wang, S.-F., Zhang, H., Jarosinski, J., Gorczakowski, A. and Podfilipski, J., Laminar burning velocities and Markstein lengths of premixed methane/air

flames near the lean flammability limit in microgravity. *Combust. Flame*, **157**, pp. 667-675, 2010.
[12] Halter, F., Tahtouh, T. and Mounaim-Rousselle, C., Nonlinear effects of stretch on flame front propagation. *Combust. Flame*, **157**, pp. 1825-1832, 2010.
[13] Bosschaart, K.J., de Goey, L.P.H. and Burgers, J.M., The laminar burning velocity of flames propagating in mixtures of hydrocarbons and air measured with the heat flux method. *Combust. Flame*, **136**, pp. 261-269, 2004.
[14] Linteris, G.T. and Truett, L., Inhibition of premixed methane-air flames by fluoromethanes. *Combust. Flame*, **105**, pp. 15-27, 1996.
[15] Williams, F.A., *Combustion Theory*, 2nd ed., Benjamin/Cummings: Menlo Park, CA, pp. 415-423, 1985.
[16] Law, C.K., Dynamics of stretched flames. *Proc. Combust. Inst.*, **22**, pp. 1381-1402, 1988.
[17] Wu, C.K. and Law, C.K., On the determination of laminar flame speeds from stretched flames. *Proc. Combust. Inst.*, **20**, pp. 1941-1949, 1984.
[18] Vagelopoulos, C.M., Egolfopoulos, F.N. and Law, C.K., Further considerations on the determination of laminar flame speeds with the counterflow twin-flame technique. *Proc. Combust. Inst.*, **25**, pp. 1341-1347, 1994.
[19] Egolfopoulos, F.N., Zhang, H. and Zhang, Z., Wall effects on the propagation and extinction of steady, strained, laminar premixed flames. *Combust. Flame*, **109**, pp. 237-252, 1997.
[20] Law, C.K., Zhu, D.L. and Yu, G., Propagation and extinction of stretched premixed flames. *Proc. Combust. Inst.*, **21**, pp. 1419-1426, 1986.
[21] San Diego Mechanism Homepage, http://web.eng.ucsd.edu/mae/groups/combustion/mechanism.html [cited 1 December 2005].
[22] Davis, S.G., Law, C.K. and Wang, H., Propene pyrolysis and oxidation kinetics in a flow reactor and laminar flames. *Combust. Flame*, **119**, pp. 375-399, 1999, also see http://ignis.usc.edu/Mechanisms/C3/c3.html.
[23] Chen, Z.H., Lin, T.H. and Sorab, S.H., Combustion of liquid fuel spray in stagnation-point flow. *Combust. Sci. Tech.*, **60**, pp. 63-77, 1988.
[24] Markstein, G.H., Experimental and theoretical studies of flame front stability. *J. Aerospace Sci.*, **18**, pp. 199-209, 1951.
[25] Clavin, P., Dynamic behavior of premixed flame fronts in laminar and turbulent flows. *Prog. Energy Combust. Sci.*, **11**, pp. 1-59, 1985.